Developmental Biology 394 (2014) 228–241

Contents lists available at ScienceDirect

Developmental Biology

journal homepage: www.elsevier.com/locate/developmentalbiology

The FgfrL1 receptor is required for development of slow muscle fibers

Ruth Amann [a], Stefan Wyder [b], Anne M. Slavotinek [c], Beat Trueb [a,d,*]

[a] Department of Clinical Research, University of Bern, 3010 Bern, Switzerland
[b] Institute of Plant Biology, University of Zurich, 8008 Zurich, Switzerland
[c] Department of Pediatrics, University of California, San Francisco, CA 94143-0748, USA
[d] Department of Rheumatology, University Hospital, 3010 Bern, Switzerland

ARTICLE INFO

Article history:
Received 12 March 2014
Received in revised form
13 August 2014
Accepted 16 August 2014
Available online 27 August 2014

Keywords:
Fibroblast growth factor
Fibroblast growth factor receptor
Fgfr
FgfrL1
Diaphragm
Extraocular muscles
Slow muscle fibers
Muscle development

ABSTRACT

FgfrL1, which interacts with Fgf ligands and heparin, is a member of the fibroblast growth factor receptor (Fgfr) family. FgfrL1-deficient mice show two significant alterations when compared to wildtype mice: They die at birth due to a malformed diaphragm and they lack metanephric kidneys. Utilizing gene arrays, qPCR and in situ hybridization we show here that the diaphragm of FgfrL1 knockout animals lacks any slow muscle fibers at E18.5 as indicated by the absence of slow fiber markers Myh7, Myl2 and Myl3. Similar lesions are also found in other skeletal muscles that contain a high proportion of slow fibers at birth, such as the extraocular muscles. In contrast to the slow fibers, fast fibers do not appear to be affected as shown by expression of fast fiber markers Myh3, Myh8, Myl1 and MylPF. At early developmental stages (E10.5, E15.5), FgfrL1-deficient animals express slow fiber genes at normal levels. The loss of slow fibers cannot be attributed to the lack of kidneys, since Wnt4 knockout mice, which also lack metanephric kidneys, show normal expression of Myh7, Myl2 and Myl3. Thus, FgfrL1 is specifically required for embryonic development of slow muscle fibers.

Introduction

The diaphragm is a sheet of skeletal muscle that separates the thoracic cavity from the abdominal cavity. Its major function is to enable respiration. When the diaphragm contracts, the volume of the thoracic cavity increases and air is drawn into the lungs. During embryonic development, the diaphragm forms from the pleuroperitoneal fold, a wedge-shaped tissue that extends from the lateral cervical wall to the esophageal mesentery and the septum transversum (Babiuk et al., 2003; Merrell and Kardon, 2013). Between stages E12.5 and E15.5 in the mouse, the pleuroperitoneal fold is invaded by myoblast precursor cells that originate from the cervical somites C3, C4 and C5. The cells proliferate and migrate to all regions of the diaphragm, except the central tendinous sheet and the tendinous zone between the costal and crural region, which remain amuscular. After a few rounds of proliferation, the myoblasts align and fuse to myotubes that give rise to primary muscle fibers. Between E16.5 and E18.5, a second wave of myoblast precursors invades the diaphragm and contributes to the formation of secondary myofibers. At this time point, the mouse embryo starts to actively contract the diaphragm muscle.

Similar to all other skeletal muscles, the diaphragm is composed of slow, oxidative and fast, glycolytic muscle fibers (Schiaffino and Reggiani, 2011). This diversification of fiber types is already observed early during development and appears to reflect an intrinsic heterogeneity of myoblast cell lineages. The fiber types differ not only by their energy metabolism (oxidative or glycolytic), but also by the composition of myofibrillar proteins (Biressi et al., 2007). Today, the best markers for the different fiber types are the isoforms of the myosin heavy chains. The mouse genome harbors 11 genes for sarcomeric myosin heavy chains, 6 of which are expressed in most skeletal muscles, while the other 5 are only expressed in highly specialized muscles. Myh1, Myh2 and Myh4 are transcribed in adult fast fibers, Myh3 (Myh-emb) is found in embryonic fast fibers, Myh8 (Myh-neo) in fetal fast fibers, and Myh7 is expressed in all slow muscle fibers (Schiaffino and Reggiani, 2011).

Muscle fibers originating from the first wave of myoblast migration express mainly Myh3 and Myh7 until developmental stage E16. At E16 some of these fibers lose Myh7 expression and begin to transcribe the Myh8 gene. As a consequence, fibers expressing Myh3 and Myh7 will later give rise to slow muscle fibers, whereas fibers expressing Myh3 and Myh8 will form fast fibers (Schiaffino and Reggiani, 2011). Secondary muscle fibers that

* Corresponding author at: Department of Clinical Research, University of Bern, Murtenstrasse 35, 3010 Bern, Switzerland.
E-mail address: beat.trueb@dkf.unibe.ch (B. Trueb).

http://dx.doi.org/10.1016/j.ydbio.2014.08.016

form during the second wave of myoblast migration express primarily Myh3 and Myh8, but not Myh7, although in slow muscles there is a tendency to transcribe Myh7 as well. The molecular basis for the switch from the slow to the fast muscle phenotype is not well understood and in spite of many efforts, only little progress has been made in its elucidation (Kelly and Buckingham, 2000; Schiaffino and Reggiani, 2011). It appears that transcription factors of the Six family control the fast gene program since double knockout mice deficient in Six1 and Six4 show specific downregulation of fast muscle fibers (Richard et al., 2011). The transcriptional repressor Sox6 is also involved since Sox6-deficient mice show downregulation of fast fibers and upregulation of slow fibers (Hagiwara et al., 2007). The transcription factor Nfix appears to control the switch from the embryonic to the adult muscle program, as Myh7 is upregulated in embryonic muscles of Nfix knockout mice but downregulated in Nfix overexpressing mice (Messina et al., 2010). This effect is mediated by members of the transcription factor family NFAT, which control Myh7 expression and which are regulated in a negative way by Nfix (Calabria et al., 2009).

After birth and in the adult animal, skeletal muscles have the capacity to undergo adaptive changes in fiber types according to alterations in innervation, mechanical loading and hormonal control. Some details are known about these adaptive changes after birth. Slow muscle fibers differ from fast fibers in their intracellular calcium concentration. The calcium-dependent regulatory proteins calmodulin kinase (CaMK) and calcineurin phosphatase specifically control the slow phenotype. Furthermore, members of the nuclear factor receptors PPAR and PGC1α are involved as well (Schiaffino and Reggiani, 2011).

We have been studying for some time the structure and function of a novel growth factor receptor termed FgfrL1 (Trueb, 2011). This receptor interacts with heparin and Fgf ligands similar to the classical fibroblast growth factor receptors Fgfr1-Fgfr4 (Beenken and Mohammadi, 2009). However, it cannot transduce the signal to the interior of the cell by transphosphorylation because it lacks the intracellular tyrosine kinase domain. It has therefore been speculated that FgfrL1 may act as a decoy receptor that binds and neutralizes Fgf ligands (Sleeman et al., 2001; Trueb et al., 2003). To analyze the function of FgfrL1 during embryonic development, we have generated knockout mice with a specific disruption of the FgfrL1 gene (Baertschi et al., 2007). These knockout mice develop quite normally until birth, but die immediately after delivery. The reason for the perinatal lethality is a malformation of the diaphragm muscle, which remains too weak to inflate the lungs after birth. The FgfrL1-deficient diaphragm shows only about 60% of the thickness of the wildtype diaphragm and some portions of the muscle, especially the dorsal and most ventral areas of the costal muscles, are reduced or completely missing. Other skeletal muscles such as the muscles of the limbs do not appear to be affected. The molecular reason for the diaphragm malformation is not known but we have demonstrated that it is not related to alterations in innervation or to differences in the expression of the myogenic regulatory factors MyoD, Myf5, Mrf4 and myogenin (Baertschi et al., 2007).

In addition to the malformed diaphragm, our knockout mice also show a nearly complete lack of the metanephric kidneys (Gerber et al., 2009). The molecular mechanism for this malformation has been studied in some detail. At E10, the ureteric bud invades the metanephric mesenchyme and starts to branch in a stereotypic fashion as in control animals. After one or two rounds of branching, differentiation stops and no conversion of the metanephric mesenchyme into epithelial renal vesicles and nephrogenic structures takes place. Gene expression studies demonstrated that the alterations in the FgfrL1-deficient kidneys are caused by the specific downregulation of Wnt4, Lhx1 and Fgf8, three molecular regulators that are known to be essential for the development of the metanephric kidneys (Gerber et al., 2009).

Here we set out to analyze the molecular reasons for the malformation of the diaphragm muscle. We show that the diaphragm of FgfrL1 null mice specifically loses its slow muscle fibers and that this change may account for the size reduction of the respiratory muscle. Thus, FgfrL1 is required for embryonic development of slow muscle fibers.

Materials and methods

Transgenic animals

FgfrL1$^{-/-}$ mice were originally described by Baertschi et al. (2007). Wnt4$^{-/-}$ mice (129-Wnt4tmAmc/EiJ) have been produced by Stark et al. (1994) and were obtained through The Jackson Laboratory, Bar Harbor, Maine (USA). Heterozygous mouse lines were kept at the local animal facility according to the relevant national guidelines (approval number BE 84/12). FgfrL1$^{-/-}$ and Wnt4$^{-/-}$ animals were bred by back crossing of heterozygous mice. For an exactly timed pregnancy, the noon of the day, at which a vaginal plug was detected, was counted as E0.5. Embryos from the same litter were used for all comparative studies of wildtype and knockout animals.

RNA and quantitative PCR

Total RNA was extracted from freshly dissected tissues or from tissues kept in RNA-later by the GeneElute miniprep kit from Sigma-Aldrich Co. (St. Louis MO, USA). The RNA was transcribed into first strand cDNA by reverse transcriptase from Moloney Murine Leukemia Virus (ImProm-II, Promega, Madison WI, USA). Primers for selected gene transcripts (Table S1) were designed by the Probe Library Tool from Roche Diagnostics (Rotkreuz, Switzerland) and ordered from Microsynth (Balgach, Switzerland). The transcript levels were quantified by real time PCR utilizing Sybrgreen and an ABI 7500 Fast platform (Applied Biosystems).

Northern blot

Northern blotting was done as previously described (Baertschi et al., 2007). Total RNA was separated on a 1% agarose gel in the presence of formaldehyde and transferred to a Nylon membrane by vacuum blotting. The blot was hybridized under standard conditions with probes that had been radiolabeled with [α-^{32}P]-dCTP.

Gene arrays

Two types of microarrays were used for differential gene profiling. Probes from diaphragms were analyzed on GeneChip Mouse Gene 1.0 ST Arrays (Affymetrix, Santa Clara CA, USA). These chips contained 750,000 unique oligonucleotides covering more than 28,000 murine genes (LopezJimenez et al., 2010). Probes from eyes were analyzed on Agilent gene expression arrays (Whole Mouse Genome Microarray 4 × 44,000, G4122F). In either case, three individual RNA preparations from wildtype and three individual RNA preparations from knockout mice were separately transcribed into labeled cDNAs utilizing original chemicals from the corresponding supplier of the chips. Microarrays were subjected to hybridization with the labeled probes, followed by extensive washing according to the instructions of the manufacturers. Signals were extracted from the final images using Affymetrix Power Tools and Agilent Feature Extraction software, respectively. Data analysis was performed on the R platform for

statistical computing with packages from the Bioconductor project (Gentleman et al., 2004). Gene annotation and identifier conversions were retrieved from the Mouse Genome Database (http://www.informatics.jax.org).

In situ hybridization

In situ hybridization was performed on thin sections as previously described (Trueb et al., 2003). Anti-sense and sense riboprobes were transcribed in the presence of ^{35}S-UTP with RNA polymerase T7 and T3, respectively, from a pSK+ vector that contained the mouse cDNA sequence (AJ293947, nucleotides 661-1417). After hybridization and stringent washing, the sections were coated with Kodak NTB-2 emulsion and exposed for 3 days at 4 °C. The signal was developed with D-19 developer (Eastman Kodak Co.) and the sections were stained with H&E.

Whole mount in situ hybridization was performed following the protocol of Piette et al. (2008) with minor modifications described on the GUDMAP gene expression database (http://www.gudmap.org/Research/Protocols/McMahon.html). Briefly, samples were fixed overnight with 4% paraformaldehyde in PBS containing 0.1% Tween 20 (PBSTW). The tissues were dehydrated through a graded series of methanol (25%, 50%, 75%, 100%) in PBSTW and then stored at −20 °C. Samples were rehydrated, bleached for 30 min with 6% hydrogen peroxide and digested with proteinase K (10 μg/ml, 15–30 min). After another cycle of fixation with 0.2% glutaraldehyde/4% paraformaldehyde in PBSTW, the tissues were prehybridized in hybridization buffer (50% formamide, 5x saline sodium citrate, 1% SDS, 50 μg/ml yeast t-RNA, 50 μg/ml heparin) and hybridized overnight at 68 °C with various digoxigenin-labeled riboprobes (see below). After a round of extensive washing steps, the sections were blocked with 3% bovine serum albumin in Tris buffered saline containing 0.1% Triton X-100 and incubated overnight at 4 °C with an anti-digoxigenin antibody (alkaline phosphatase-conjugated Fab fragments from Roche, 1:2000). Following several rounds of washing, the hybridization signal was developed with BM Purple containing 1 mM Levamisole (Roche).

Specific probes for whole mount in situ hybridization were prepared by PCR with cDNA derived from various mouse tissues and the primer pairs listed in Table S2. Amplified products were subcloned into the vector pSPT19 (Roche). Riboprobes were transcribed from the linearized vectors using the DIG RNA labeling kit (SP6/T7) from Roche.

Apoptosis

Two complementary tests were used to detect programmed cell death; the Lysotracker system that stains acidic organelles in living cells (Zucker et al., 1999) and the caspase-3 system that identifies activated caspase-3 with a specific antibody. Embryos were dissected from the mother together with the amniotic sac and immediately placed into Hank's balanced salt solution (HBSS) kept at 37 °C. The diaphragms were then isolated one after the other from the embryos and incubated in the dark in HBSS containing 5 μM Lysotracker Red DND-99 (Molecular Probes, Invitrogen). After 30 min, the samples were extensively washed with HBSS and fixed overnight at 4 °C with 4% paraformaldehyde in PBS. The fixative was removed by washing with PBS and the specimens were dehydrated through a graded series of methanol. Stained diaphragms were transferred into the wells of special depression slides (Thermo Scientific, 0.6–0.8 mm depression) and embedded with aqueous mounting agent (Aquatex, Merck Millipore).

For caspase-3 staining, freshly dissected diaphragms were fixed in 4% formaldehyde/PBS at room temperature. After 15 min, the fixative was removed by extensive washing with PBS and unspecific sites were blocked for 60 min with PBS containing 5% BSA, 0.3% Triton X-100. The samples were incubated overnight at 4 °C with a monoclonal rabbit antibody against cleaved caspase-3 (5A1E, Cell Signaling Technology Inc.) in PBS containing 1% BSA, 0.3% Triton X-100. After extensive washing, the samples were incubated for 2 h at room temperature in the same buffer with a Rhodamine labeled secondary antibody (Sigma). Following a final round of washing, the diaphragms were mounted in depression slides as described above.

Immunohistochemistry

Diaphragms were dissected and immediately fixed with 4% formaldehyde in PBS for 20 min. The samples were dehydrated by passing them through a series of ethanol, isopropanol and xylol and subsequently embedded in paraffin (Shandon Citadel 1000 Tissue Processor, Thermo Fisher Scientific). Sections of 5 μm were cut and rehydrated in xylol, ethanol and PBS. To unmask antigenic determinants, the sections were heated for 30 min to 95 °C in 10 mM citric acid, pH 6.0. Cell membranes were permeabilized with 0.025% Triton X-100 in Tris-buffered saline for 10 min and unspecific sites were blocked with 3% bovine serum albumin in the same buffer for 2 h. Incubation with anti-Myh7 (MyHCI) antibody (clone NOQ7.5.4D, 1:800, Sigma) was performed at 37 °C for 2 h. Bound antibodies were visualized with Cy3-conjugated goat anti-mouse IgG at RT for 2 h (Jackson Laboratories Inc., 1:50). Finally, the specimens were mounted with Aquatex (Merck) and inspected under a microscope equipped with epi-fluorescence optics (Nikon Eclipse E800).

To determine the thickness of the diaphragms as well as the ratio of fibers and nuclei per area, cryosections were prepared as previously described (Baertschi et al., 2007). The sections were stained with TRITC-conjugated wheat germ agglutinin (WGA, Sigma, 10 μg/ml) and DAPI (4′,6-diamidino-2-phenylindole, 1 μg/ml) for 30 min at RT. After extensive washing, the sections were mounted as described above.

Results

Expression of FgfrL1 in the diaphragm

As a first step, we checked expression of FgfrL1 in the diaphragm of wildtype mice. By Northern blotting (Fig. 1A), we detected FgfrL1 mRNA during the entire development of the diaphragm, from E14.5 when myoblasts precursor cells are known to migrate into the diaphragm and to fuse to primary myofibers, until E19.5 when a second wave of myoblast precursors had just invaded the diaphragm and started to fuse to secondary myofibers. We noted a slight increase of FgfrL1 expression towards later stages. However, a similar increase was also observed with the internal marker Gapdh, suggesting that diaphragms at later stages were transcriptionally more active than those at earlier stages and consequently contained a higher proportion of mRNAs relative to ribosomal RNAs.

To investigate the spatial distribution of expression, we performed in situ hybridization with E17.5 diaphragms utilizing a radiolabeled anti-sense probe for FgfrL1. Under dark field optics, we observed a fairly even distribution of silver grains (indicative of FgfrL1 mRNA) throughout the costal muscle (Fig. 1B). When the sections were stained by H&E and inspected under bright field optics, fine dots of silver grains were found on all striated muscle fibers. No regions of muscle fibers that would specifically lack any silver grains could be observed. Control sections hybridized in parallel with a sense probe for FgfrL1 did not reveal any signal.

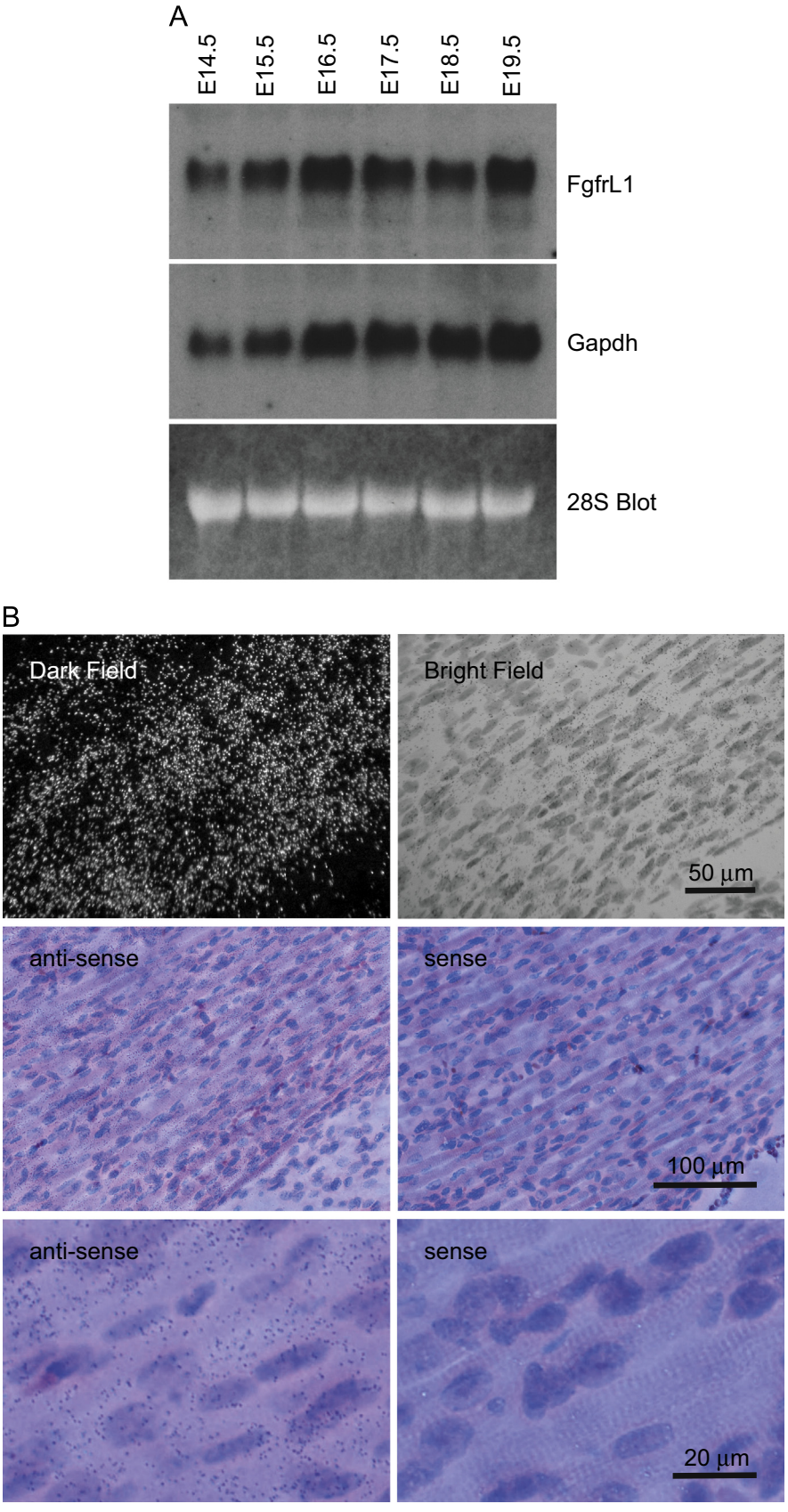

Fig. 1. Expression of FgfrL1 in the diaphragm of wildtype mice during embryonic development analyzed by Northern blotting (A) and by in situ hybridization (B). (A) Total RNA (7 µg) from mouse diaphragms of E14.5 to E19.5 was separated on a 1% agarose gel, transferred to a Nylon membrane and hybridized successively with radiolabeled probes specific to FgfrL1 and Gapdh, respectively. As a loading control, the 28S ribosomal RNA stained with ethidium bromide after transfer to the membrane is included. (B) Cryosections of E17.5 diaphragms were hybridized with a radiolabeled probe for FgfrL1. The hybridization signal was inspected under dark field and bright field optics as indicated. All of the cross-striated muscle fibers reacted with the probe as demonstrated by distribution of silver grains on all H&E stained muscle fibers. Barely any signal was detected on control sections hybridized with the corresponding sense probe.

Taken together, the Northern blotting experiment and the in situ hybridization results suggest that all muscle fibers of the developing diaphragm, slow as well as fast fibers, express the FgfrL1 gene.

Transcription profile of FgfrL1-deficient skeletal muscles

To get an idea why the diaphragm muscle is severely reduced in FgfrL1-deficient mice, we used gene arrays and compared the expression levels of approximately 28,000 genes between normal and FgfrL1$^{-/-}$ diaphragms at developmental stage E18.5 (Fig. 2A). We found 8 transcripts that were significantly downregulated (3–10 fold) in the FgfrL1 null diaphragm, whereas no transcript was significantly upregulated (Table 1). It therefore appears that the loss of FgfrL1 was not compensated by the upregulation of another gene product. Interestingly, the best 4 downregulated hits (Myl2, Myl3, Tpm3, Myh7) coded for typical constituents of slow muscle fibers that normally are not found in fast fibers. These results suggest that the FgfrL1-deficient diaphragm specifically lacks the slow muscle fibers.

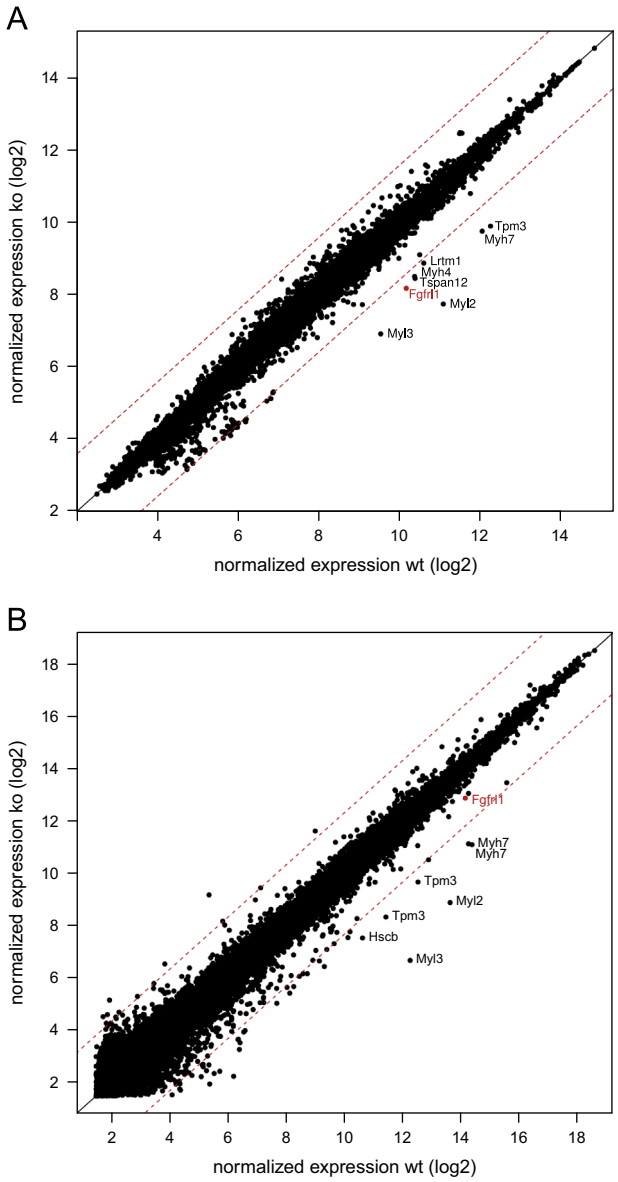

Fig. 2. Identification of transcripts that are differentially expressed in FgfrL1-deficient diaphragms (A) and eyes (B) at E18.5. The scatter plots show average normalized signal intensities from three independent experiments using samples from wildtype and FgfrL1 knockout mice. Each dot represents an individual gene. Dashed lines correspond to a fold change of 3 (A) and 5 (B). Some transcripts are labeled by their gene symbols.

Table 1
Gene transcripts downregulated in FgfrL1-deficient muscles.

Diaphragm muscle		Extraocular muscles (Eye)	
Gene	Fold change wt/ko	Gene	Fold change wt/ko
Myl2	10.1	Myl3	47.8
Myl3	6.1	Myl2	26.6
Tpm3	5.1	Myh7	8.7
Myh7	4.9	Tpm3	8.5
FgfrL1	4.0	Hscb	8.5
Myh4	3.7	Myh6	5.9
Tspan12	3.7	Calcr	4.5
Lrtm1	3.3	Tnnt1	4.2

A myosin molecule of slow muscle fibers consists of two identical heavy chains (encoded by Myh7), one regulatory light chain (Myl2) and one essential light chain (Myl3) (Schiaffino and Reggiani, 2011; Hernandez et al., 2007). On the other hand, myosin molecules of fast fibers contain primarily heavy chains of type Myh3 (embryonic) or Myh8 (neonatal) and light chains of type Myl1 (essential) and MylPF (regulatory) at E18.5. Expression of the latter transcripts characteristic of fast muscle fibers was barely affected in the FgfrL1 knockout diaphragm. Myh3 was regulated by a factor of 1.13, Myh8 by 1.05, Myl1 by 1.06 and MylPF by 1.05.

Tpm3, which was significantly reduced in the FgfrL1$^{-/-}$ diaphragm similar to Myh7, Myl2 and Myl3, also occurs exclusively in slow muscle fibers (Schiaffino and Reggiani, 2011). Tpm1 and Tpm2 are found in fast fibers. Again, the expression levels of Tpm1 and Tpm2 were barely affected in the FgfrL1-deficient diaphragm (1.03 and 1.05-fold, respectively). These results strongly suggest that only the slow muscle fibers are reduced in the knockout diaphragm whereas the fast fibers persist at normal levels.

The results of the gene array were verified by RT-PCR, using Gapdh as standard to normalize the expression levels between wildtype and knockout diaphragms. These experiments confirmed that the levels of Myh7, Myl2 and Myl3 were significantly reduced in the FgfrL1-deficient diaphragm (up to 10-fold), while those of Myh3, Myh8, Myl1 and MylPF were barely affected (Fig. 3A). As expected, expression of FgfrL1 was virtually absent in the knockout diaphragm, while the levels of two control genes, namely Wnt4 and RpS9, were barely affected.

Next, we investigated whether the downregulation of the slow muscle transcripts was specific to the diaphragm muscle or whether it might also be observed with other muscle types. To this end, we analyzed the soleus muscle at E18.5 by qPCR. In fact, we could confirm a similar downregulation of Myh7 in the soleus, but the results varied considerably between individual samples (Fig. 3B), probably because the soleus muscle contains a relatively small proportion of slow to fast muscle fibers at this developmental stage (Agbulut et al., 2003). We therefore focused on another muscle type that should contain a high amount of slow muscle fibers at E18.5, the extraocular muscles of the eye (Porter et al., 2001; Kjellgren et al., 2003). Eyes of FgfrL1 knockout animals were isolated and vitreous as well as lens were removed. Such preparations should contain 6 extraocular muscles as well as sclera, cornea and retina of the eye, which were not removed due to the small size at this developmental stage. A gene array was hybridized with probes generated from this material. We obtained results very similar to those observed with the diaphragm (Fig. 2B). Barely any transcripts were upregulated in the knockout eyes and only 8 transcripts were significantly downregulated

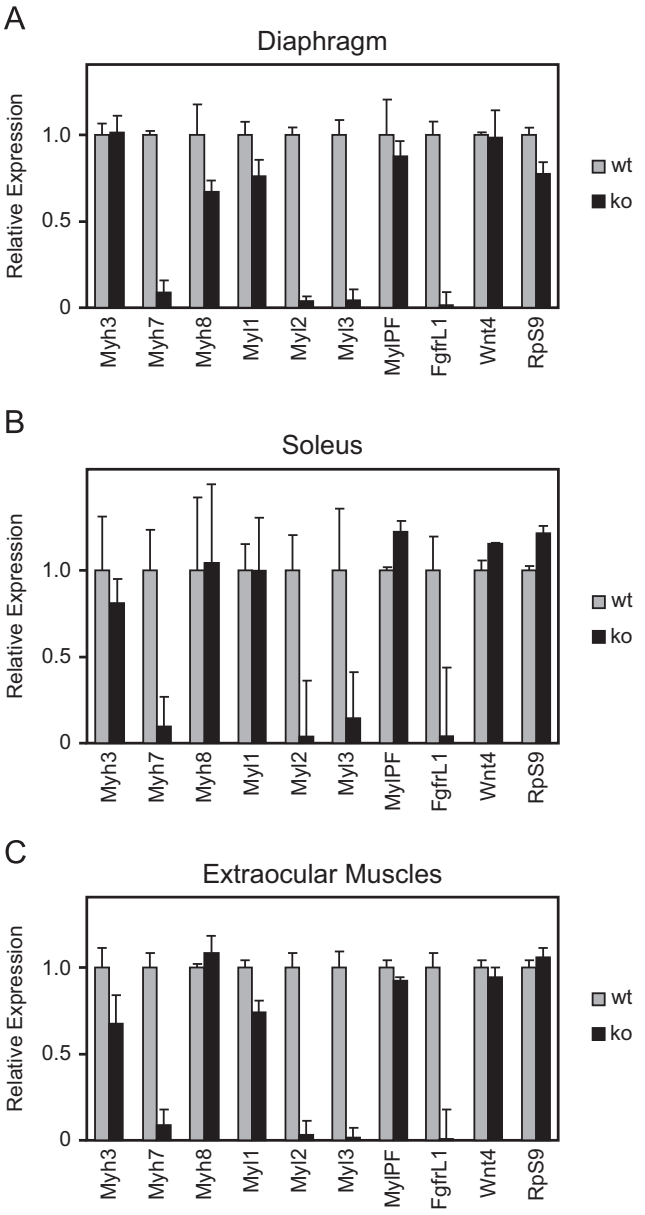

Fig. 3. Verification of differential gene expression in FgfrL1-deficient diaphragms (A), soleus (B) and extraocular muscles (C) at E18.5 by quantitative PCR. RNA samples were transcribed into cDNAs and quantified by PCR using the primer pairs given in Table S1. The bars show normalized expression levels relative to Gapdh from triplicates with standard errors. Grey bars represent levels in wildtype mice, black bars levels in FgfrL1 knockout mice. Markers for slow muscle fibers (Myh7, Myl2 and Myl3) are downregulated in the FgfrL1-deficient tissues, while markers for fast, embryonic muscle fibers (Myh3, Myh8, Myl1 and MylPF) persist at normal levels. Rps9 is another gene frequently used for normalization.

(Table 1). Again, the 4 best hits coded for typical slow muscle proteins, including Myl3, Myl2, Myh7 and Tpm3, and expression of fast muscle genes was barely affected. RT-PCR further confirmed these results (Fig. 3C). Myh7, Myl2 and Myl3 were strongly downregulated, while Myh3, Myh8, Myl1 and MylPF were barely affected. Taken together, our results suggest that slow muscle fibers are specifically lost in most, if not all, muscle types of FgfrL1 knockout mice.

Spacial distribution of muscle markers by in situ hybridization

To get some information about the spatial distribution of the different muscle fibers, we performed in situ hybridization experiments. Since individual fibers cannot be visualized over their entire length on thin sections, we turned to whole mount in situ hybridization and used a protocol originally developed for entire mouse embryos (Piette et al., 2008). With a probe for Myh7, this technique allowed clear visualization of slow muscle fibers in wildtype diaphragms at E18.5 (Fig. 4). A strong signal was observed in costal, crural as well as intercostal muscles. At higher magnification, individual muscle fibers could be traced along their total length. Approximately every third muscle fiber was stained, alternating with unstained (probably fast) fibers, yielding a zebra-like pattern. Very rarely two positive fibers touched each other. With diaphragms of FgfrL1-deficient mice, we did not observe such a pattern. Staining was extremely weak and the signal was mostly confined to the intercostal muscles. At higher magnification, the costal muscles had a translucent appearance and showed only occasional, faintly positive fibers. Hybridization with a probe for Myh3 (specific to embryonic fast muscle fibers) yielded a much stronger signal. As shown at higher magnification, the majority of all muscle fibers were stained. Utilizing this Myh3 probe, a similar distribution was also found with diaphragms of FgfrL1-deficient animals. This result confirms our previous observation that the FgfrL1$^{-/-}$ diaphragm lacks slow muscle fibers, while embryonic fast fibers are present.

Analogous results were obtained with probes for Myl3, the essential light chain of slow fibers, and Myl1, the essential light chain of fast fibers (Fig. 4). Signal for Myl3 was found in approximately 30% of all muscle fibers from wildtype animals, but it was absent from the diaphragm of knockout animals. On the other hand, staining for Myl1 was found in the majority of the fibers from both wildtype and knockout tissues. Taken together, these results corroborate our findings obtained by microarrays and qPCR that the FgfrL1-deficient diaphragm is devoid of slow muscle fibers.

Loss of slow fibers during embryonic development

Next we investigated whether the signal for marker genes of slow muscle fibers could be traced down at earlier developmental stages. We checked embryos, again by whole mount in situ hybridization, at E10.5, a stage at which expression of muscle genes is known to be confined to the somites (Fig. 5). In fact, we detected relatively strong staining of Myh7 transcripts in all somites of wildtype embryos. However, to our surprise, Myh7 staining was also observed at this stage in FgfrL1-deficient animals and revealed no difference when compared to wildtype animals. Moreover, when the diaphragm was inspected at E15.5, we also detected expression of Myh7 in the FgfrL1-deficient tissues. At this stage, a fairly strong signal was observed in the costal and intercostal muscles, even in the knockout animals. Thus, the Myh7 gene is faithfully expressed in the diaphragm muscle of early knockout animals but expression is lost later during development.

We therefore used qPCR and analyzed the temporal expression of Myh7 as a marker for slow fibers and Myh3 as a marker for embryonic fast fibers between E15.5 and E19.5 (Fig. 6). In fact, we observed a dramatic decline of the Myh7 levels in the knockout diaphragms. At E15.5, the level of Myh7 was even higher in the knockout than in the wildtype diaphragm, probably due to some compensatory effects, but at E16.5 the level in the knockout diaphragm dropped below that of the wildtype. At E17.5, expression of Myh7 was barely detectable in the knockout diaphragm, while expression of Myh3 persisted throughout development from E15.5 to E19.5. Thus, our FgfrL1-deficient animals are able to express Myh7 at early stages. However, expression stalls at E16.5 while expression of the other myosin heavy chains continues.

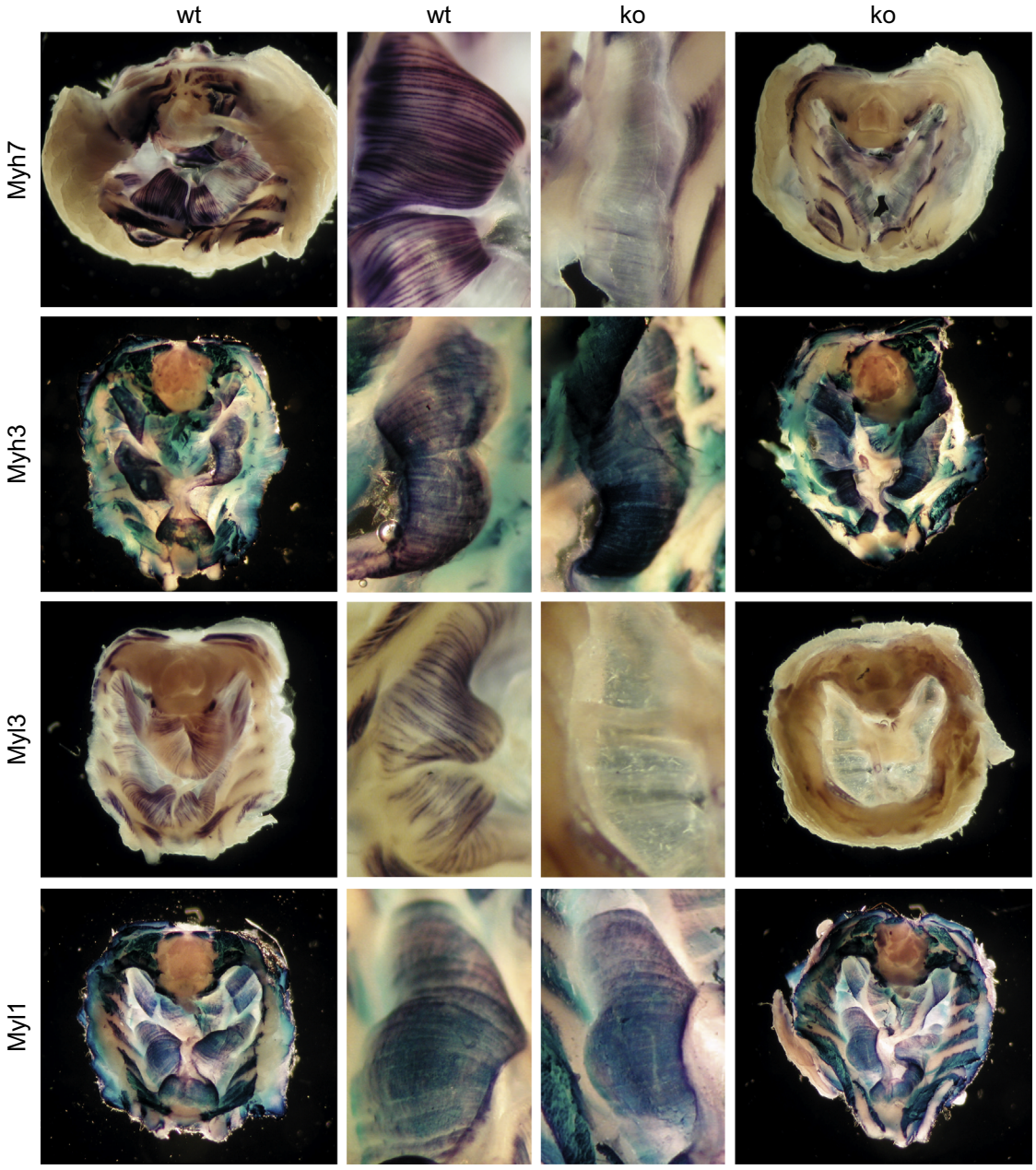

Fig. 4. Whole mount in situ hybridization of selected marker genes on E18.5 diaphragms. Samples from wildtype and FgfrL1-deficient mice were hybridized with digoxigenin labeled RNA probes. The probes were detected with an alkaline phosphatase-conjugated antibody against digoxigenin. The smaller panels show higher power magnifications of selected regions from the larger panels. Probes specific to slow muscles (Myh7, Myl3) stain almost exclusively fibers of the wildtype samples, while probes for fast muscles (Myh3, Myl1) also stain fibers of the knockout samples.

Increased apoptosis in knockout diaphragms

One reason why the number of slow muscle fibers might decrease during development could be programmed cell death. During the apoptotic process, cells shrink, nuclei fragment and cellular debris becomes engulfed by neighboring cells. This phagocytotic process correlates with acidification and increased lysosomal activity of the tissue. We therefore used the lysosomal dye Lysotracker to investigate cell death in knockout diaphragms between E16.5 and E18.5. In fact, incubation of freshly dissected knockout diaphragms with Lysotracker demonstrated increased cell death, as indicated by the occurrence of numerous red dots along muscle fibers when compared to wildtype diaphragms (Fig. 7A). When treated in parallel, wildtype diaphragms were nearly devoid of any acidic red dots.

Our results were further confirmed with an antibody against activated caspase-3, a key enzyme of the apoptotic process. Activation of caspase-3 requires proteolytic processing of the inactive zymogen to the activated enzyme. In fact a monoclonal antibody specific to cleaved caspase-3 revealed increased apoptosis in knockout samples of E16.5–E18.5 when compared to wildtype samples (Fig. 7B). Wildtype diaphragms showed hardly any positive reaction with this antibody, while knockout diaphragms had multiple positive dots along the muscle fibers. Cell death appeared to be slightly stronger at E16.5 than at E18.5 as shown by the increased number of red dots at the earlier stage.

To verify a decrease of muscle fibers by independent means, we measured the thickness of the diaphragm muscle and determined the number of fibers and nuclei per area. For this purpose, cryosections of diaphragms from wildtype and knockout animals

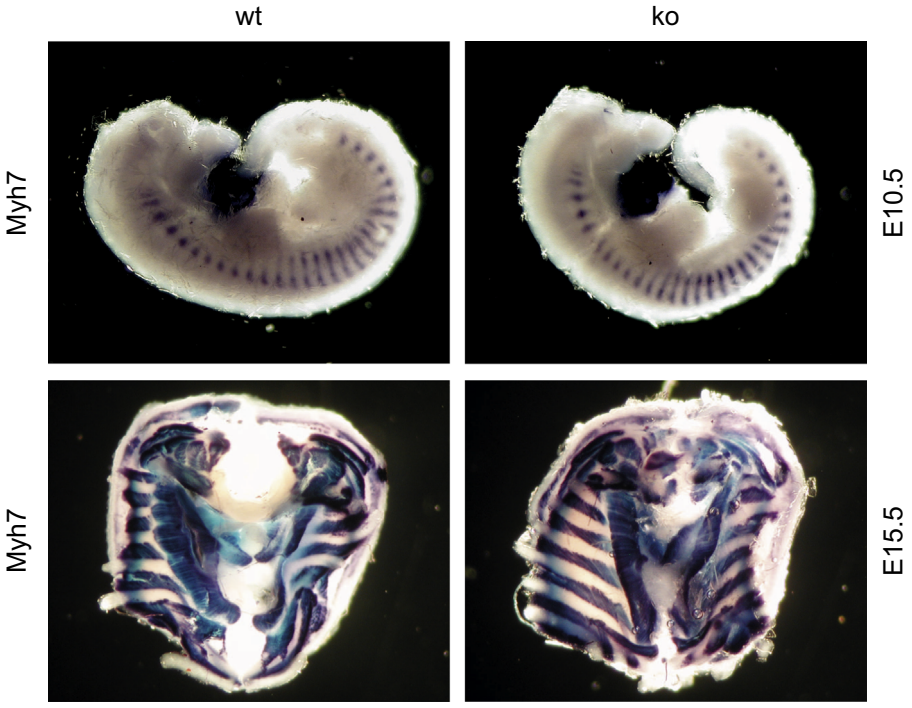

Fig. 5. Whole mount in situ hybridization of Myh7 on samples from wildtype and FgfrL1-deficient mice. Entire embryos of E10.5 and E11.5 as well as diaphragms of E15.5 were hybridized with a digoxigenin labeled RNA probe and the signal was detected with an alkaline phosphatase-conjugated antibody. The probe stains the somites of early embryos as well as costal and intercostal muscles of E15.5 diaphragms in both wildtype and FgfrL1-deficient samples. Similar results were also obtained with embryos of E11.5 and a probe for Myl3 (not shown).

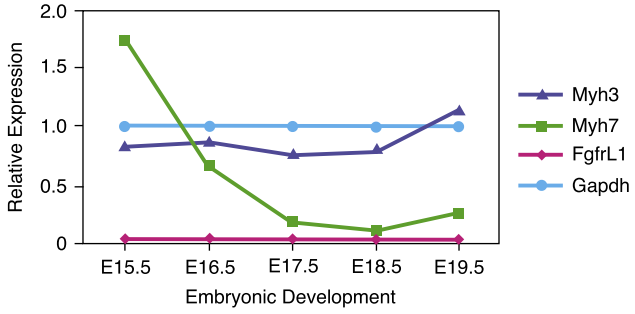

Fig. 6. Time course of the relative expression levels (ko/wt) of several marker genes in FgfrL1-deficient diaphragms. Expression of Myh7 as a marker for slow muscle fibers and Myh3 as a marker for fast embryonic muscle fibers were quantified by PCR. Gapdh was used for normalization. FgfrL1 is not expressed in the knockout diaphragm. Expression levels of Myh7 (ko/wt) are high at E15.5 but decrease dramatically after E16.5, while expression levels of Myh3 (ko/wt) stay nearly constant throughout embryonic development.

at E18.5 were stained with wheat germ agglutinin, a lectin that binds to carbohydrates of basement membrane proteins, thereby marking the boundaries of individual muscle fibers. At the same time the nuclei were stained with DAPI (Fig. 8). We found that FgfrL1-deficient diaphragms were about 35% thinner than wildtype diaphragms (wildtype 183 ± 6 µm, knockout 120 ± 5 µm, $p < 0.001$ Student's t test) in keeping with our previous results. However, knockout diaphragms contained a similar number of nuclei/mm^2 to wildtype diaphragms (wildtype 6253 ± 236 nuclei/mm^2, knockout 6603 ± 351 nuclei/mm^2). Furthermore, knockout diaphragms had a similar number of fibers/mm^2 (wildtype 4092 ± 179 fibers/mm^2, knockout 4248 ± 255 fibers/mm^2). Thus, FgfrL1-deficient diaphragms showed a reduction of about 30% in the total number of nuclei and fibers in comparison to wildtype diaphragms. It is of interest to note that FgfrL1-deficient diaphragms also had an uneven, wrinkled appearance with bumps and scar-like lesions (Figs. S1 and S2) in contrast to wildtype diaphragms that were much smoother. Taken together with the results of the apoptosis tests, our observations are consistent with the hypothesis that programmed cell death is involved in the loss of slow muscle fibers at late embryonic stages.

Verification at the protein level

To confirm downregulation of slow muscle fibers at the protein level, we used a monoclonal antibody against Myh7 (MyHCI) on paraffin sections (Fig. 9). At E18.5, this antibody reacted with approximately 20% of all muscle fibers of the diaphragm from wildtype animals, demonstrating the specificity of the antibody. With sections from knockout animals that had been treated in parallel under identical conditions, overall staining was much weaker. Only very few fibers reacted with the antibody and the staining intensity of these fibers was clearly reduced, suggesting that part of the slow muscle fibers were in the process of losing Myh7 (MyHCI) expression. In sharp contrast, incubation of sections from diaphragms at E15.5 with the same antibody produced a strong signal with both wildtype and knockout samples. At this developmental stage, individual myoblasts are known to fuse to myotubes and primary myofibers as outlined in the introduction. We found that most of the elongated (fused) myofibers reacted with the anti-Myh7 (MyHCI) antibody, while single myoblasts were clearly negative. Importantly, there was no obvious difference between wildtype and knockout samples in terms of staining intensity. These experiments demonstrate that Myh7 is expressed at the protein level at an early developmental stage (E15.5), but lost at a later stage (E18.5). Thus, our observations made by in situ hybridization and qPCR are fully confirmed at the protein level by indirect immunofluorescence.

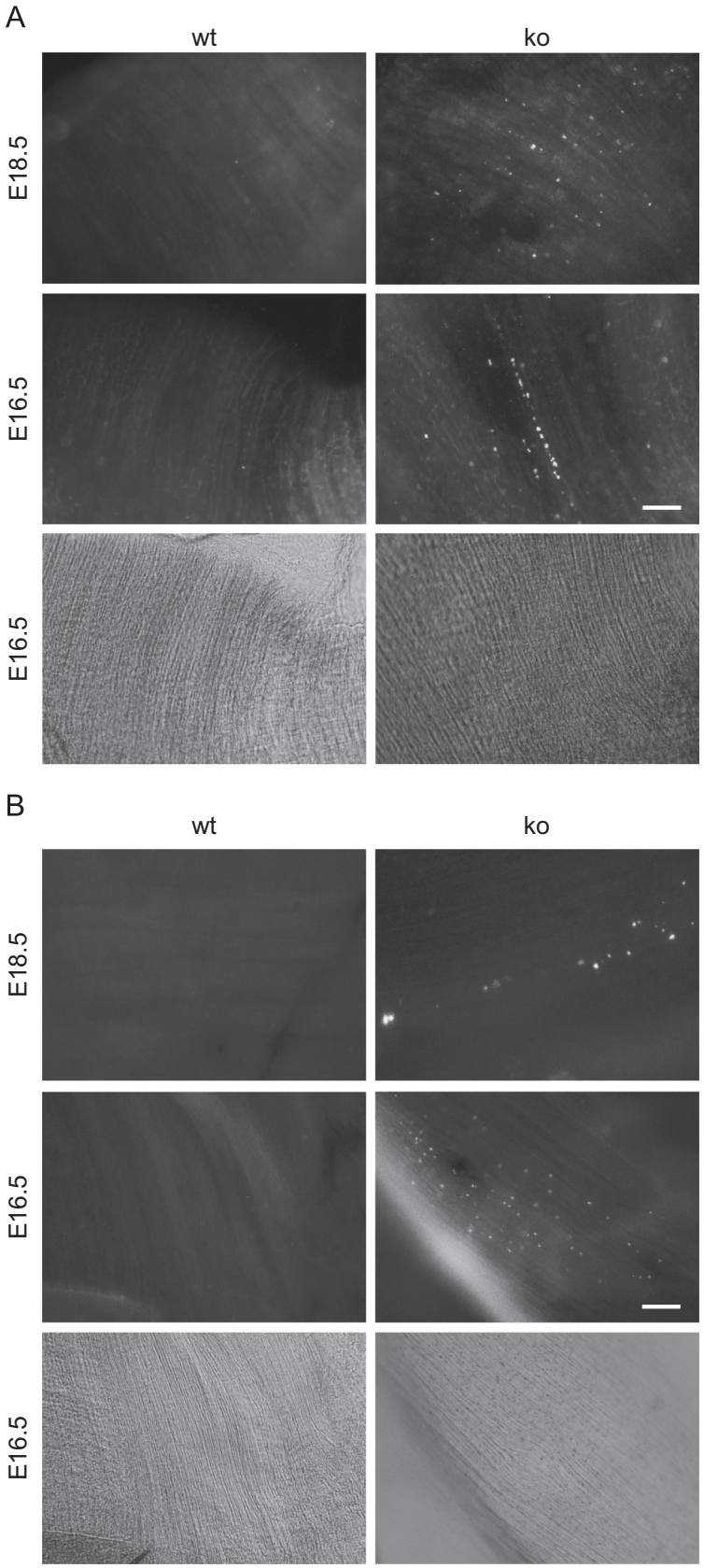

Fig. 7. Detection of cell death in diaphragms from FgfrL1-deficient mice. (A) Diaphragms derived from wildtype and knockout mice of E18.5 and E16.5 were incubated for 30 min with Lysotracker Red DND-99. Acidic organelles indicative of cell death are observed at multiple sites along the muscle fibers of the knockout diaphragms (40–50 dots), but only at few sites in the wildtype diaphragms (1–2 dots). (B) Diaphragms from wildtype and knockout mice of E18.5 and E16.5 were fixed and incubated with an antibody against activated caspase-3, followed by a Rhodamine labeled secondary antibody. Bright dots indicative of apoptosis are only observed in the diaphragms from knockout mice (17 dots at E18.5, 45 dots at E16.5). Phase contrast images of E16.5 are included to visualize the orientation of the muscle fibers. Bar = 100 μm.

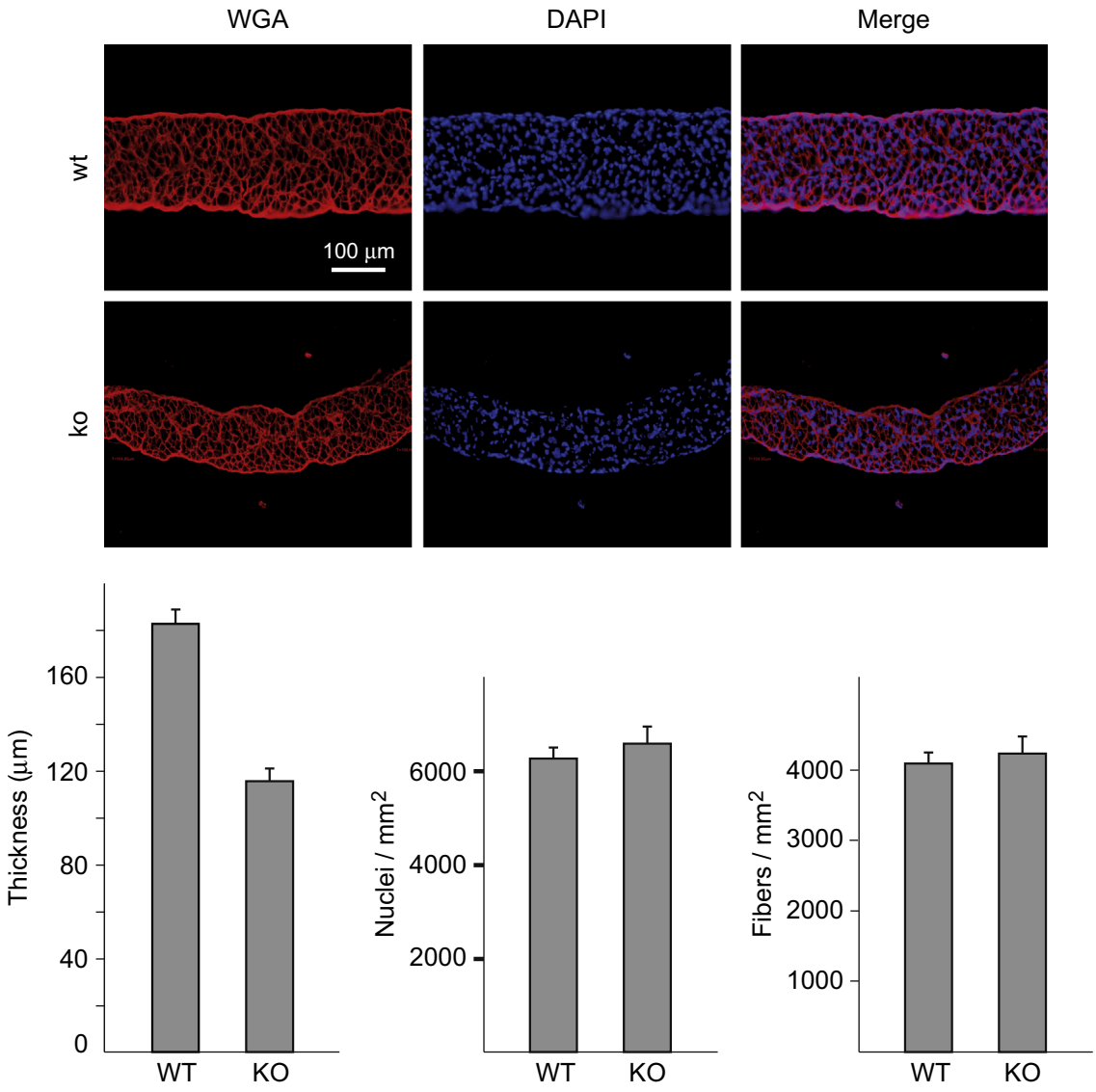

Fig. 8. Comparison of thickness as well as number of fibers and nuclei between wildtype and FgfrL1-deficient diaphragms. Cryosections of diaphragms at E18.5 were stained with wheat germ agglutinin (WGA) and DAPI in order to mark boundaries of myofibers and their nuclei, respectively. The thickness of the diaphragms and the number of nuclei and fibers per area are given by grey bars with standard error ($n=6$). Additional samples can be found in supplementary Fig. S1 and S2. FgfrL1-deficient diaphragms were 35% thinner than wildtype diaphragms, but the number of nuclei and fibers/mm^2 was comparable. Thus, FgfrL1-deficient diaphragms show a reduction in the total number of muscle fibers when compared to wildtype diaphragms.

Loss of slow fibers is not caused by the lack of kidneys

FgfrL1-deficient mice die at birth due to a malformed diaphragm muscle (Baertschi et al., 2007). However, they also lack any metanephric kidneys (Gerber et al., 2009). Theoretically, the loss of slow muscle fibers could therefore be caused indirectly by the lack of kidneys. To address this possibility, we analyzed Wnt4 knockout mice (Stark et al., 1994). Similar to FgfrL1-deficient mice, such Wnt4 knockout mice lack any metanephric kidneys (Fig. 10). In FgfrL1$^{-/-}$ as well as in Wnt4$^{-/-}$ animals, kidney development stalls around E12.5 when the metanephric mesenchyme should condense and convert into epithelial renal vesicles. As a consequence, Wnt4 and FgfrL1 knockout mice have only rudimentary structures in place of the metanephric kidneys (Fig. 10).

Homozygous Wnt4 knockout mice of E18.5 were therefore analyzed for the presence of slow muscle fibers in their diaphragm. By whole mount in situ hybridization, we detected expression of Myh7 at levels similar to those of wildtype mice (Fig. 11A). RT-PCR further confirmed that the markers of slow fibers, including Myh7, Myl2 and Myl3, were expressed at similar levels in the diaphragm of wildtype and Wnt4 knockout mice (Fig. 11B). Only the levels of FgfrL1 were reduced to 50%, probably due to some crosstalk between Fgf and Wnt signaling.

The loss of slow muscle fibers observed in FgfrL1-deficient mice can therefore not be explained by the absence of the metanephric kidneys. Rather, it must be a consequence of the missing receptor FgfrL1.

Discussion

Skeletal muscles are composed of fast, glycolytic muscle fibers, which contract quickly, and of slow, oxidative muscle fibers, which are resistant to fatigue (Schiaffino and Reggiani, 2011). Despite considerable efforts, the molecular mechanism(s) how discrimination between development of fast and slow muscle fibers is accomplished, is largely unknown.

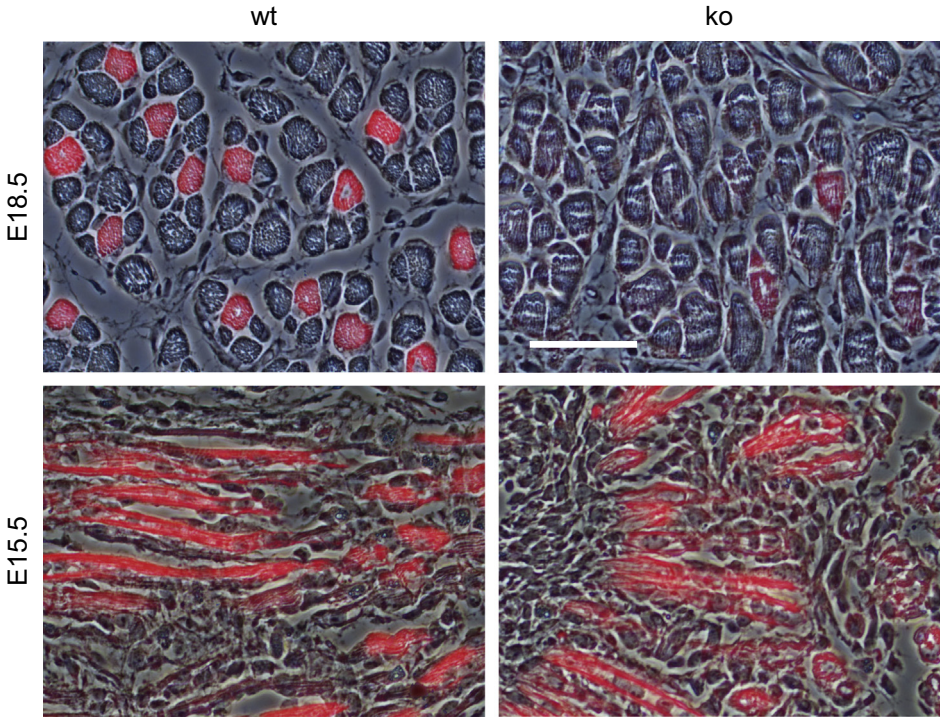

Fig. 9. Indirect immunofluorescence of diaphragms with anti-Myh7 (MyHCI) antibodies. Paraffin sections of diaphragms from wildtype and knockout animals at E18.5 and E15.5 were incubated with a monoclonal antibody against Myh7 (MyHCI), followed by a Cy3-conjugated secondary antibody. Images were taken with epifluorescence optics (red) and merged with images taken by phase contrast (grey). At E15.5, the antibody stained primarily myofibers and fused myoblasts from both wildtype and knockout animals, but it did not stain any single myoblasts. At E18.5, the antibody stained a subgroup of muscle fibers, most likely slow fibers, on sections from wildtype animals. With sections from knockout animals, the number of positive myofibers was significantly reduced at E18.5. Bar = 50 μm.

Here we demonstrated that receptor FgfrL1 is specifically required for development of slow muscle fibers. FgfrL1 knockout mice are born with a diaphragm muscle that is devoid of any slow fibers, whereas fast fibers are correctly developed. This malformation leads to perinatal death of the animals, as the diaphragm is too weak to inflate the lungs with air after birth. Other muscle types might similarly be affected but most of them contain low proportions of slow fibers at birth and consequently such differences are difficult to detect. Muscles with a high proportion of slow fibers at birth, namely the extraocular muscles, also reveal a dramatic downregulation of slow fibers in the FgfrL1$^{-/-}$ mice.

FgfrL1-deficient mice lack metanephric kidneys in addition to slow muscle fibers. Mammals can survive without functional kidneys for 1–2 days, but they cannot survive longer than a few minutes without any functional diaphragm. We showed that the loss of slow muscle fibers cannot be attributed to the lack of kidneys because Wnt4-deficient mice contain slow fibers at normal proportion although they lack metanephric kidneys similar to the FgfrL1-deficient mice. In fact, Wnt4 knockout mice die within 24 h after birth (Stark et al., 1994), while FgfrL1 knockout mice die within minutes after birth (Baertschi et al., 2007).

We further demonstrated that FgfrL1-deficient animals are able to transcribe all characteristic genes of slow fibers, such as Myh7, Myl2 and Myl3, at early developmental stages (E10.5–E15.5). However, slow fibers are specifically lost later during development (after E16.5) while fast fibers persist. Therefore, the receptor FgfrL1 is specifically required for normal development of slow muscle fibers.

In a previous publication we have obtained analogous results with the metanephric kidneys (Gerber et al., 2009). FgfrL1 knockout mice lack both kidneys because the metanephric mesenchyme cannot transform into renal epithelium, the epithelium that would later give rise to glomeruli. At that time, we showed that the induced metanephric mesenchyme of FgfrL1 null mice decays by apoptosis. It therefore appears that FgfrL1 is an important survival factor that enables differentiation and at the same time counteracts apoptosis.

A similar conclusion has also been reached in studies with Six1/Six4 double knockout mice (Grifone et al., 2005). Such mice show general muscle hypoplasia since Six1 and Six4 control early steps of myogenesis. Without the Six transcription factors, myoblast precursor cells lose their identity and die by apoptosis. It therefore appears that the myogenic program is regulated not only by cell proliferation, but to a decisive extent also by cell survival. It has been speculated that overexpression or inhibition of a single factor in a regulatory network triggers by default an apoptotic program (Clark et al., 2002). Obviously this program can be initiated at distinct hierarchical levels if different factors are missing. Six1 and Six4 are situated upstream of FgfrL1 in the hierarchy of regulatory genes that control myogenesis since these factors are expressed at normal levels in our FgfrL1 knockout mice (Gerber et al., 2012), whereas FgfrL1 is lost in Six1/Six4-deficient mice (Richard et al., 2011). The Six factors appear to control the fast muscle program (Niro et al., 2010), while FgfrL1 primarily controls the slow muscle program. However, in either case targeted disruption of these regulatory factors may lead to apoptosis, although at different stages of embryonic development.

We can only speculate about the exact molecular mechanism(s), by which FgfrL1 might control development of slow muscle fibers. We showed that the levels of the myogenic regulatory factors (MyoD, Myf5, Myogenin, Mrf4) and myocyte enhancer factors (Mef2A, Mef2B, Mef2C and Mef2D) are not altered in our knockout mice (Baertschi et al., 2007). Likewise, we did not observe any changes in the innervation of the diaphragm by the phrenic nerve. Moreover, transcription of several other regulators, including Sox6, FoxO1, calcineurin, Fgf3, Fgf8, and Wnt4, is not altered in the mutant diaphragms when compared to wildtype diaphragms as shown by microarrays and qPCR (Fig. 2 and unpublished observation). It is obvious that FgfrL1 cannot signal by its own as it lacks the

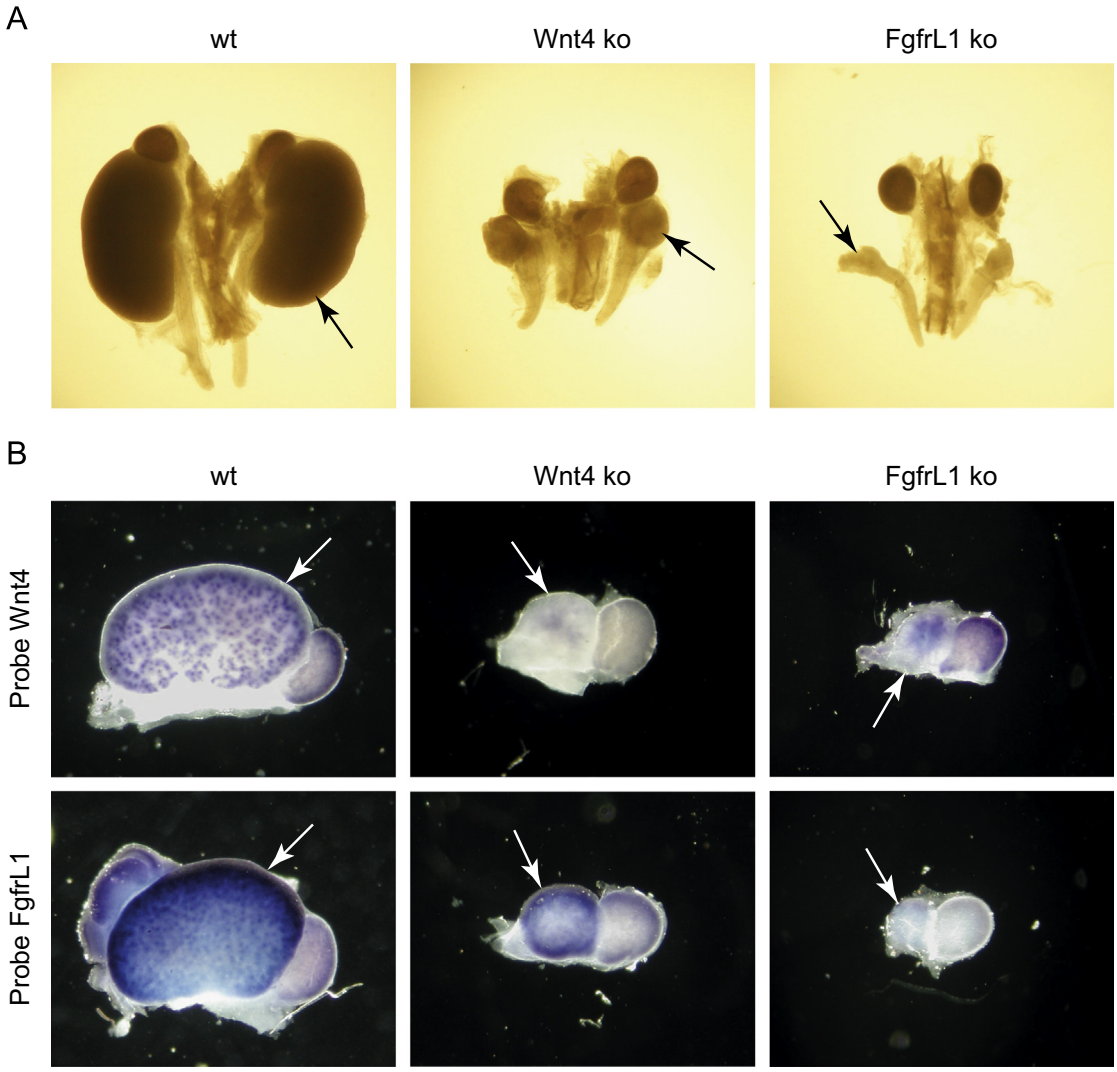

Fig. 10. Comparison of kidneys from Wnt4- and FgfrL1-deficient mice. (A) Wnt4-deficient mice possess only rudimentary structures in place of the metanephric kidneys at E18.5, similar to FgfrL1 knockout mice. (B) Kidneys of E15.5 were hybridized with probes specific to FgfrL1 and Wnt4, as indicated in the left margin. FgfrL1 is expressed in the kidney rudiments of Wnt4-deficient mice, Wnt4 is expressed in the kidney rudiments of FgfrL1-deficient mice. Arrows point to the metanephric kidneys.

intracellular tyrosin kinase domain. It is therefore conceivable that the effects of FgfrL1 are accomplished by the extracellular domain of the protein, which is known to promote cell–cell adhesion. In fact, FgfrL1 is usually observed at cell–cell contact sites (Rieckmann et al., 2008). When coated on plastic surfaces, it induces robust adhesion of various cell types such as 3T3 fibroblasts and C2C12 myoblasts. This adhesion promoting activity could be attributed to the Ig2 domain of the FgfrL1 molecule that is known to interact with heparan sulfate chains as they occur in glypican-4 and -6 (Steinberg et al., 2010). FgfrL1 might therefore promote cell adhesion and block apoptosis similar to other cell adhesion proteins, including fibronectin, laminin and integrin. The term anoikis has been coined to describe apoptosis induced by inappropriate cell–matrix interactions (Frisch and Screaton, 2001; Gilmore, 2005). As such an adhesion factor, FgfrL1 might represent one of the key proteins that are required for condensation of the metanephric mesenchyme and its conversion into renal epithelia during kidney development. Likewise, it could be one of the crucial cell surface receptors that enables cell–cell recognition during alignment and fusion of myoblasts into myotubes, in particular in slow fibers. In fact, the levels of FgfrL1 are sharply upregulated when C2C12 myoblasts fuse into myotubes (Baertschi et al., 2007). We have further tackled this idea and searched for fusion defects in the myofibers of our FgfrL1 null mice. However, we could not detect any alterations in the thickness of the individual fibers or in the number of nuclei per fiber of our knockout diaphragms (Steinberg et al., 2010). Likewise, we did not observe any effects with monoclonal FgfrL1 antibodies on fusion of C2C12 myoblasts in vitro. Further experiments are therefore needed to clarify the role of FgfrL1 during myogenesis. At any rate, FgfrL1 is one of the few proteins identified today that are specifically needed for normal development of slow muscle fibers.

Acknowledgments

This work was supported by grants from the Swiss National Science Foundation (31003A-143350) and the Helmut Horten Foundation.

Appendix A. Supporting information

Supplementary data associated with this article can be found in the online version at http://dx.doi.org/10.1016/j.ydbio.2014.08.016.

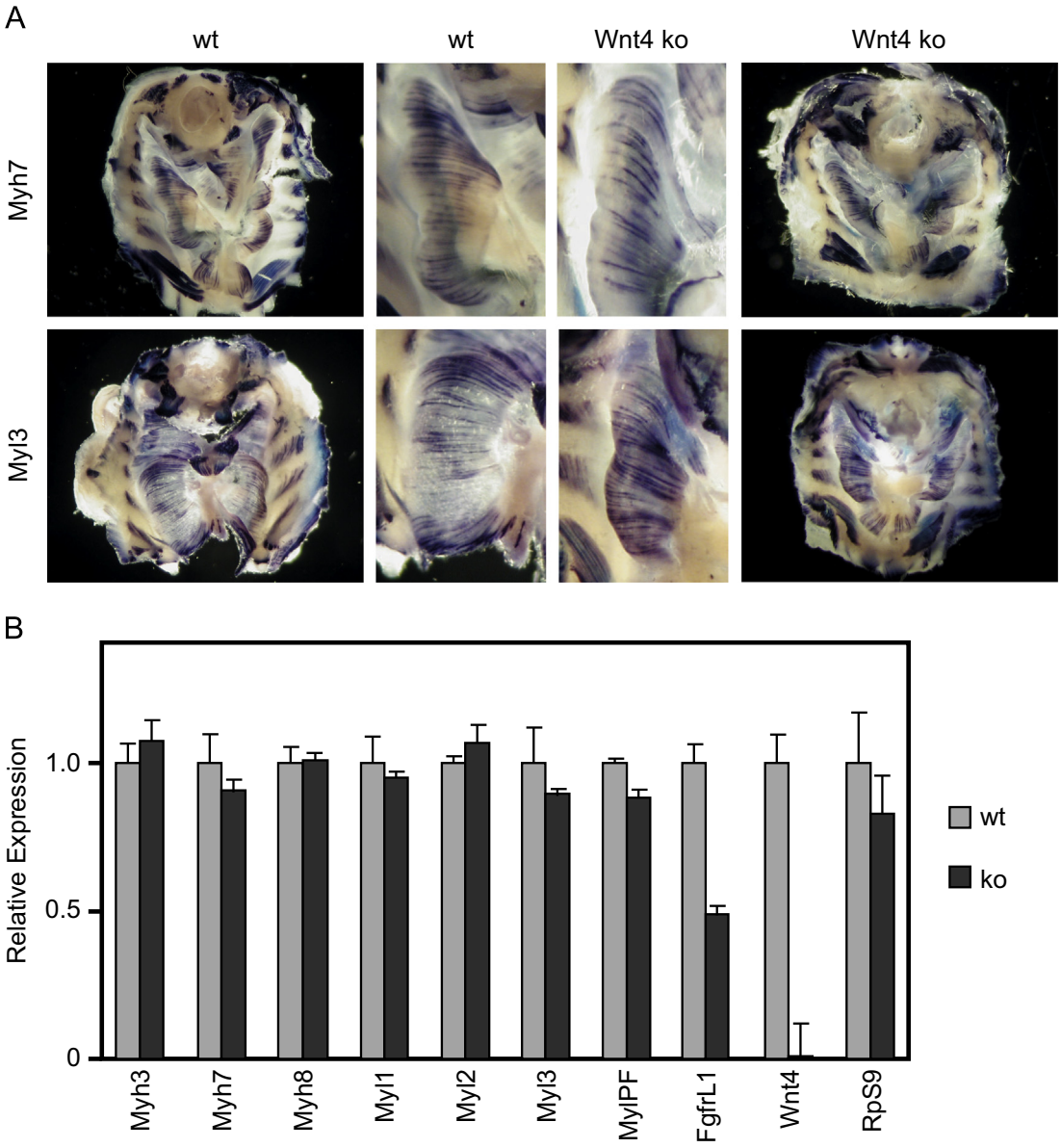

Fig. 11. Comparison of diaphragms from wildtype and Wnt4-deficient mice. (A) Diaphragms at E18.5 were hybridized with probes specific to Myh7 and Myl3 as markers for slow muscle fibers. Hybridization signal is observed in the diaphragms from both wildtype and Wnt4 knockout mice. The smaller panels give higher power magnifications of selected areas from the larger panels. (B) Confirmation of gene expression by quantitative PCR. RNA samples from Wnt4-deficient diaphragms at E18.5 were transcribed into cDNAs and quantified by PCR using the primer pairs given in Table S1. The bars show normalized expression levels relative to Gapdh from triplicates with standard error. Grey bars represent mRNA levels of wildtype mice, black bars those of Wnt4 knockout mice. Markers for slow muscle fibers (Myh7, Myl2, Myl3) and markers for fast muscle fibers (Myh3, Myh8, Myl1, MylPF) are expressed at similar levels in both wildtype and knockout animals.

References

Agbulut, O., Noirez, P., Beaumont, F., Butler-Browne, G., 2003. Myosin heavy chain isoforms in postnatal muscle development of mice. Biol. Cell 95, 399–406.

Babiuk, R.P., Zhang, W., Clugston, R., Allan, D.W., Greer, J.J., 2003. Embryological origins and development of the rat diaphragm. J. Comp. Neurol. 455, 477–487.

Baertschi, S., Zhuang, L., Trueb, B., 2007. Mice with a targeted disruption of the Fgfrl1 gene die at birth due to alterations in the diaphragm. FEBS J. 274, 6241–6253.

Beenken, A., Mohammadi, M., 2009. The FGF family: biology, pathophysiology and therapy. Nat. Rev. Drug Discovery 8, 235–253.

Biressi, S., Molinaro, M., Cossu, G., 2007. Cellular heterogeneity during vertebrate skeletal muscle development. Dev. Biol. 308, 281–293.

Calabria, E., Ciciliot, S., Moretti, I., Garcia, M., Picard, A., Dyar, K.A., Pallafacchina, G., Tothova, J., Schiaffino, S., Murgia, M., 2009. NFAT isoforms control activity-dependent muscle fiber type specification. Proc. Nat. Acad. Sci. U.S.A. 106, 13335–13340.

Clark, S.W., Fee, B.E., Cleveland, J.L., 2002. Misexpression of the eyes absent family triggers the apoptotic program. J. Biol. Chem. 277, 3560–3567.

Frisch, S.M, Screaton, R.A., 2001. Anoikis mechanisms. Curr. Opin. Cell Biol. 13, 555–562.

Gentleman, R.C., Carey, V.J., Bates, D.M., Bolstad, B., Dettling, M., Dudoit, S., Ellis, B., Gautier, L., Ge, Y., Gentry, J., Hornik, K., Hothorn, T., Huber, W., Iacus, S., Irizarry, R., Leisch, F., Li, C., Maechler, M., Rossini, A.J., Sawitzki, G., Smith, C., Smyth, G., Tierney, L., Yang, J.Y.H., Zhang, J., 2004. Bioconductor: open software development for computational biology and bioinformatics. Genome Biol. 5, R80.

Gerber, S.D., Steinberg, F., Beyeler, M., Villiger, P.M., Trueb, B., 2009. The murine Fgfrl1 receptor is essential for the development of the metanephric kidney. Dev. Biol. 335, 106–119.

Gerber, S.D., Amann, R., Wyder, S., Trueb, B., 2012. Comparison of the gene expression profiles from normal and FgfrL1 deficient mouse kidneys reveals downstream targets of Fgfrl1 signaling. PLoS One 7, e33457.

Gilmore, A.P., 2005. Anoikis. Cell Death Differ. 12, 1473–1477.

Grifone, R., Demignon, J., Houbron, C., Souil, E., Niro, C., Seller, M.J., Hamard, G., Maire, P., 2005. Six1 and Six4 homeoproteins are required for Pax3 and Mrf expression during myogenesis in the mouse embryo. Development 132, 2235–2249.

Hagiwara, N., Yeh, M., Liu, A., 2007. Sox6 is required for normal fiber type differentiation of fetal skeletal muscle in mice. Dev. Dyn. 236, 2062–2076.

Hernandez, O.M., Jones, M., Guzman, G., Szczesna-Cordary, D., 2007. Myosin essential light chain in health and disease. Am. J. Physiol. Heart Circ. Physiol 292, H1643–H1654.
Kelly, R.G., Buckingham, M.E., 2000. Modular regulation of the MLC1F/3F gene and striated muscle diversity. Microsc. Res. Tech. 50, 510–521.
Kjellgren, D., Thornell, L.-E., Andersen, J., Pedrosa-Domellöf, F., 2003. Myosin heavy chain isoforms in human extraocular muscle. Invest. Ophthalmol. Vis. Sci. 44, 1419–1425.
LopezJimenez, N., Gerber, S., Popovici, V., Mirza, S., Copren, K., Ta, L., Shaw, G.M., Trueb, B., Slavotinek, A.M., 2010. Examination of FGFRL1 as a candidate gene for diaphragmatic defects at chromosome 4p16.3 shows that Fgfrl1 null mice have reduced expression of Tpm3, sarcomere genes and Lrtm1 in the diaphragm. Hum. Genet. 127, 325–336.
Merrell, A.J., Kardon, G., 2013. Development of the diaphragm—a skeletal muscle essential for mammalian respiration. FEBS J. 280, 4026–4035.
Messina, G., Biressi, S., Monteverde, S., Magli, A., Cassano, M., Perani, L., Roncaglia, E., Tagliafico, E., Starnes, L., Campbell, C.E., Grossi, M., Goldhamer, D.J., Gronostajski, R.M., Cossu, G., 2010. Nfix regulates fetal-specific transcription in developing skeletal muscle. Cell 140, 554–566.
Niro, C., Demignon, J., Vincent, S., Liu, Y., Giordani, J., Sgarioto, N., Favier, M., Guillet-Deniau, I., Blais, A., Maire, P., 2010. Six1 and Six4 gene expression is necessary to activate the fast-type muscle gene program in the mouse primary myotome. Dev. Biol. 338, 168–182.
Piette, D., Hendrickx, M., Willems, E., Kemp, C.R., Leyns, L., 2008. An optimized procedure for whole-mount in situ hybridization on mouse embryos and embryoid bodies. Nat. Protocols 3, 1194–1201.
Porter, J.D., Khanna, S., Kaminski, H.J., Rao, J.S., Merriam, A.P., Richmonds, C.R., Leahy, P., Li, J., Andrade, F.H., 2001. Extraocular muscle is defined by a fundamentally distinct gene expression profile. Proc. Nat. Acad. Sci. U.S.A. 98, 12062–12067.
Richard, A.-F., Demignon, J., Sakakibara, I., Pujol, J., Favier, M., Strochlic, L., Le Grand, F., Sgarioto, N., Guernec, A., Schmitt, A., Cagnard, N., Huang, R., Legay, C., Guillet-Deniau, I., Maire, P., 2011. Genesis of muscle fiber-type diversity during mouse embryogenesis relies on Six1 and Six4 gene expression. Dev. Biol. 359, 303–320.
Rieckmann, T., Kotevic, I., Trueb, B., 2008. The cell surface receptor FGFRL1 forms constitutive dimers that promote cell adhesion. Exp. Cell Res. 314, 1071–1081.
Schiaffino, S., Reggiani, C., 2011. Fiber types in mammalian skeletal muscles. Physiol. Rev. 91, 1447–1531.
Sleeman, M., Fraser, J., McDonald, M., Yuan, S., White, D., Grandison, P., Kumble, K., Watson, J.D., Murison, J.G., 2001. Identification of a new fibroblast growth factor receptor, Fgfr5. Gene 271, 171–182.
Stark, K., Vainio, S., Vassileva, G., McMahon, A.P., 1994. Epithelial transformation of metanephric mesenchyme in the developing kidney regulated by Wnt-4. Nature 372, 679–683.
Steinberg, F., Gerber, S., Rieckmann, T., Trueb, B., 2010. Rapid fusion and syncytium formation of heterologous cells upon expression of the FGFRL1 receptor. J. Biol. Chem. 285, 37704–37715.
Trueb, B., 2011. Biology of FGFRL1, the fifth fibroblast growth factor receptor. Cell. Mol. Life Sci. 68, 951–964.
Trueb, B., Zhuang, L., Taeschler, S., Wiedemann, M., 2003. Characterization of FGFRL1, a novel fibroblast growth factor (FGF) receptor preferentially expressed in skeletal tissues. J. Biol. Chem. 278, 33857–33865.
Zucker, R.M., Hunter III, E.S., Rogers, J.M., 1999. Apoptosis and morphology in mouse embryos by confocal laser scanning microscopy. Methods 18, 473–480.